# Structural and Dynamic Properties of Water on the GaN Polar Surface

**ARTICLE** *in* THE JOURNAL OF PHYSICAL CHEMISTRY C · OCTOBER 2011

Impact Factor: 4.77 · DOI: 10.1021/jp2070166



**4 AUTHORS**, INCLUDING:

Michael C. H. Wu
Iowa State University
**7** PUBLICATIONS **45** CITATIONS

SEE PROFILE

THE JOURNAL OF PHYSICAL CHEMISTRY C

ARTICLE

pubs.acs.org/JPCC

# Structural and Dynamic Properties of Water on the GaN Polar Surface

Osbert Zheng Tan,* K. H. Tsai, Michael C. H. Wu, and Jer-Lai Kuo*

Institute of Atomic and Molecular Sciences, Academia Sinica, Taipei, Taiwan

**ABSTRACT:** The structural and dynamic properties of water on the GaN(0001) polar surface are investigated via classical molecular dynamics simulations. The interfacial molecules are observed to have enhanced structural ordering and slowed-down dynamics compared to the liquid bulk; these unique properties are evidenced in the slower reorientational relaxation, smaller diffusion constant, and longer residence lifetime for water located at the surface region up to ∼7 Å from the substrate. Further analysis of the vibrational spectra at low frequencies shows that both the hydrogen bond network bending and the hydrogen bond stretching bands at the interface shift to the blue compared to those in the bulk, due to the strong coupling between the O atom of water and the Ga sites. The distinct spectral features along with the anisotropy of the hydrogen bond distributions of the interfacial water are complex results determined by both the substrate−water and water−water interactions.

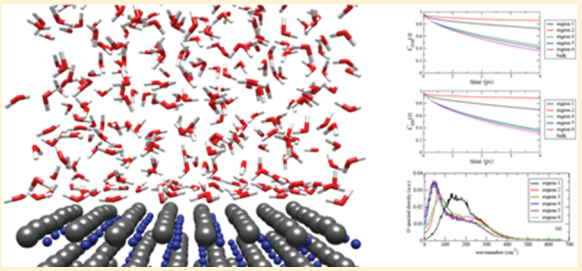

## 1. INTRODUCTION

Properties of water at the solid−liquid interface play an important role in the study of wetting, liquid nanotransportation, phase separation, heterogeneous catalysis, etc.[1−3] A number of experimental[4,5] and theoretical[6−10] research studies have provided molecular level insights into the behavior of interfacial water, where within a few molecular dimensions from the surface, the structural and dynamic properties of the interfacial water can be significantly affected by the solid substrate characteristics.[11,12]

We are focusing on the water/semiconductor interfaces here, by particularly choosing the $H_2O$/GaN system due to the technological importance of GaN and its broad applications in electronic and gas sensing devices.[13,14] The knowledge of the GaN surface characteristics and the surface interactions with the ambient molecules (particularly water) thus would be essential for the comprehension of the device operation principles,[15,16] especially when the semiconductor is exposed to the humid environment. It is of interest to see the recent investigations on the surface chemistry of water on GaN via the first principle calculations,[17−19] where on both $(10\bar{1}0)$ nonpolar and $(0001)/(000\bar{1})$ polar surfaces, water molecules are found to have the capacity to adsorb dissociatively. While in the framework of physisorption, our recent force field (FF) development and molecular dynamics (MD) simulations[20] have identified the wetting structure of water on the GaN(0001) polar surface, which is composed of a bilayer with the dipole up-and-down configurations. Along with the observations that the interfacial water would become highly patterned and very structured, it is however also interesting to know the relevant dynamic properties within the hydration layer (which is particularly defined as the wetting bilayer in this paper). The current paper will especially focus on the reorientational, translational, and residence properties of the interfacial molecules within the surface ∼10 Å region from the substrate, and their corresponding vibrational spectra and hydrogen bond (HB) distributions as a result of the strong interfacial couplings. By illustrating the local dynamics of water on this semiconductor surface, our research can be linked to the photoelectrolysis experiments conducted in the GaN/electrolyte cell for the $H_2$ generation purpose,[21−23] as the interfacial water properties are substantial to understand the counterion accumulation and the formation of the electric double layer.[24]

The remainder of this paper is organized as follows. Section 2 describes the computational methods we use in the classical MD simulations. Section 3 gives the results and discussion on different structural and dynamic properties of interfacial water on the GaN(0001) surface, including the HB density profile, radial distribution functions (RDF), residence correlation functions (RCF), in-plane mean square displacements (MSD), reorientational relaxations, and vibrational spectroscopies. A concluding remark is drawn in section 4.

## 2. COMPUTATIONAL DETAILS

We are using the FF parametrized in ref 20 to describe the $H_2O$/GaN system, where water molecules are simulated by the simple point charge model with flexible extension[25,26] (SPC-F), a modified universal force field (UFF) is employed to model the GaN polar surface, and the interactions between $H_2O$ and GaN are given by the Buckingham potentials which are fitted to the first principle binding energy hypersurface.

MD simulation is performed in GULP[27] by using the Ewald summation scheme for the electrostatics. As shown in Figure 1, the system comprises 680 water molecules with thickness around 42 Å sandwiched between two GaN polar surface slabs, where the number of water molecules is designed to fill in a volume

**Received:** July 22, 2011
**Revised:** October 11, 2011
**Published:** October 12, 2011





dx.doi.org/10.1021/jp2070166 | J. Phys. Chem. C 2011, 115, 22444–22450

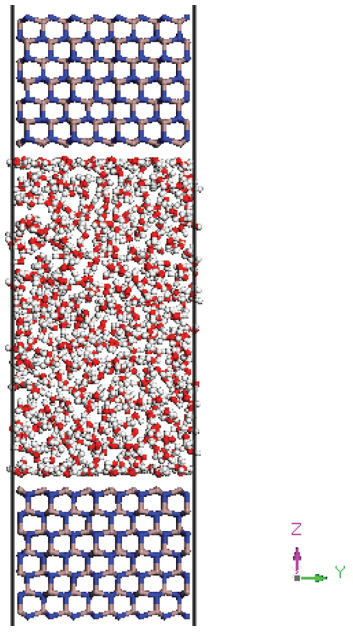


**Figure 1.** Model system for the MD simulation of water sandwiched between GaN polar surface slabs. Brown, blue, white, and red spheres represent Ga, N, H, and O atoms, respectively.

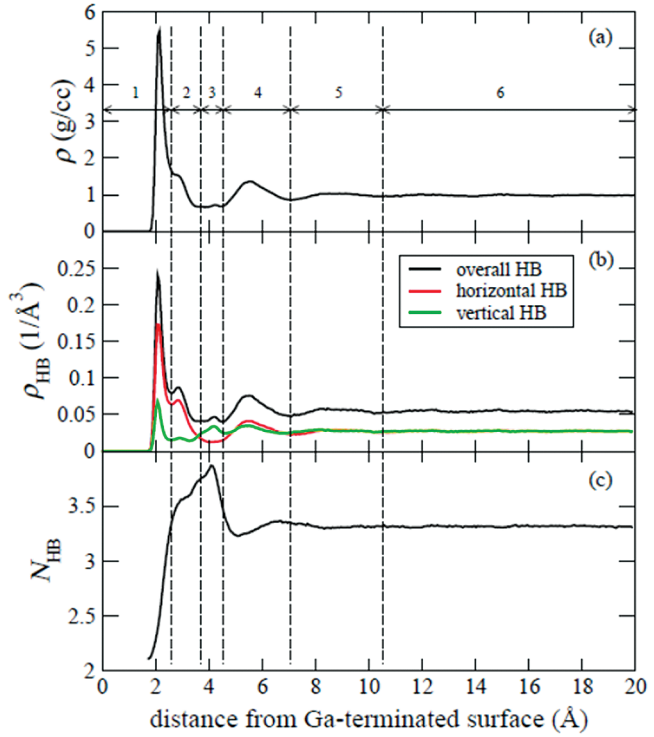


**Figure 2.** (a) Density profile of water on the lower GaN surface, where the origin is chosen to be the mean position of Ga in the top layer during the MD. (b) HB number density profile and the relevant decompositions into horizontally and vertically aligned HB number density profiles. (c) Profile of coordination number averaged on each water molecule. In all the figures, a bin size of 0.0625 Å is used. The boundaries specified by dashed vertical lines between the regions 1−2, 2−3, 3−4, 4−5, and 5−6 are located at 2.78, 3.84, 4.47, 7.09, and 10.41 Å, respectively.

corresponding to the experimental density of liquid water (∼1 g/cm$^3$). Each slab contains seven atomic double layers (ADLs) along the (0001) orientation, and at both interfaces water molecules are facing the Ga-terminated surfaces. We are using an orthorhombic supercell with the surface area designed to be 22.10 × 22.33 Å$^2$. The bottom one layer of both GaN slabs is fixed to mimic the bulk solid substrate, while the remaining six layers are fully relaxed during the MD and interact with the $H_2O$ molecules. The two N-faced pseudosurfaces are separated around 67 Å in the periodic boundary condition. The MD is carried in a NVT ensemble at 300 K. The system is initially relaxed for 0.3 ns using the velocity scaling scheme, and the data are collected in the following 1.7 ns using the Nose−Hoover thermostat. The time step is set to be 0.5 fs.

MD simulations for a bulk water reference system are also performed by using the SPC-F model. The system is composed of 768 water molecules in a 28.425 Å cubic cell (equivalent to a density of 1 g/cm$^3$) and is examined with the same ensemble, temperature, time step, etc., as in the $H_2O$/GaN calculations.

## 3. RESULTS AND DISCUSSION

**A. Structural Properties: Atomic Density and HB Density Profiles.** Figure 2a shows the atomic density profile of water on the lower GaN surface. As discussed in ref 20 a sharp concentration of molecules appear at the immediate vicinity of the surface, which is followed by a density depletion region and several residual fluctuations until it eventually converges to the bulk density value at 1 g/cm$^3$. The molecular dipole orientational profile is known to experience a damped oscillation from the surface to the bulk region, while within the first two regions molecules exhibit the most significant orientational ordering by having dipole up-and-down configurations.[20] We are following the convention in our previous studies by dividing the water film into six regions, with the six density peaks in the corresponding regions located at 2.16, 2.91, 4.22, 5.53, 8.75, and 15.21 Å, respectively (note that the second peak denotes the estimated shoulder position, the third peak indicates the little hump between region 2 and 4, and the fifth and sixth "peaks" are simply midpoint between the region boundaries). These positions will serve as the representative locations of different regions and would be used in the following analyses.

It is reported[6,8] that the structure and dynamics of interfacial water are determined by both the substrate−water and water−water interactions. Water−water interactions are largely dominated by the formation of hydrogen bonds. Figure 2b gives rise to the number density profile of HB as a function of the distance from the surface. The formation of one HB is prescribed by the geometric criterion proposed by Marti.[28] The profile is obtained by statistically summing up the HB number associated with those molecules positioned at a certain distance (molecular location determined by the O) and then dividing it by two to remove the double counting. It can be seen that the overall HB density profile is similar to the atomic density profile, by having a sharp peak at around 2.08 Å, followed by a shoulder and a small hump at region 2 and 3, and some residual fluctuations until converging in region 6. The characteristic peak positions in HB profile are basically overlapping with those in atomic density profile, demonstrating that hydrogen bonds are largely responsible for determining the structure of interfacial layers. In order to visualize the orientational anisotropy of HB in the surface region, we decompose the profile into the horizontally (in-plane) and vertically (out-of-plane) aligned HB profiles (note that the division is based on the

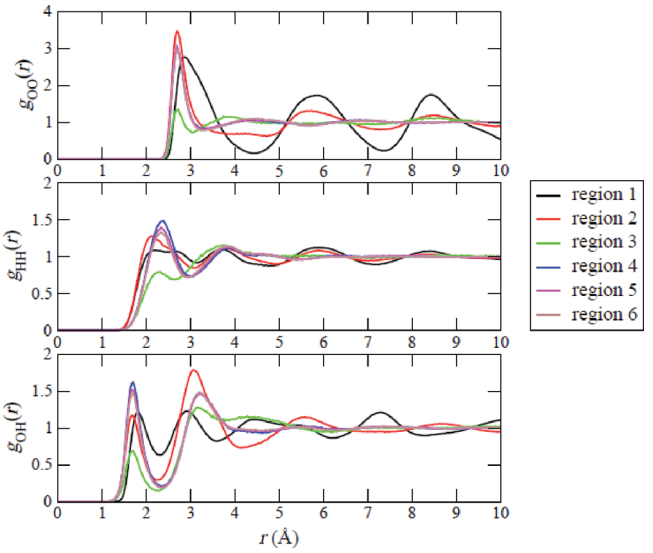


**Figure 3.** In-plane O−O, H−H, and O−H radial distribution functions in different regions.

value of $|\cos \varphi|$ that is smaller or larger than 1/2, where $\varphi$ is the polar angle of HB with respect to surface normal). From Figure 2b, it shows that within the wetting bilayer including region 1 and 2, most of the HBs are aligned horizontally; in region 3 the situation is reversed by having the HB orientation dominated by the vertical alignment. The orientational isotropy, however, is found to recover from region 4, and the profiles fluctuate in accordance with the density oscillation before the convergence in the bulk region. The anisotropy can be simply understood by the fact that the adsorbed molecules are more likely to form bonds with the neighboring molecules since bonding with the substrate is prohibited. The accumulation of the vertical HBs in the density depletion region is possibly to link the upper isotropic bulklike liquid and the bottom in-plane bonded hydration layer. The observation is consistent with the vertical alignment of molecules in region 3 where a large fraction of water coaligns its dipole with the surface normal.[20]

The coordination number (average number of HBs per water molecule) profile (Figure 2c) shows a pronounced reduction when the molecules are closer to the GaN surface, which is as expected. The profile, however, gives rise to a significant peak at region 3 by reaching 3.87 HBs per molecule, followed with a moderate depletion in region 4 before converging at regions 5 and 6. The remarkable overcoordination of molecules in region 3 compared to the bulk is unusual, since such a strongly bonded region has not been observed for water covered on other hydrophilic and hydrophobic surfaces such as silica,[11] graphene sheets,[12,29] and NaCl.[30] These nearly four coordinated molecules with dipoles vertically pointing away from the surface are expected to bridge the isotropic liquid and the anisotropic wetting layer, presumably for a smooth order transition, and they are responsible for the subtle hexagonal pattern of O in region 3 as observed in the in-plane atomic density distributions.[20] In addition, the average coordination number is 3.31 at distances larger than 10 Å from the surface, in good agreement with the coordination number (3.32) of the isotropic SPC-F bulk according to our examinations.

**B. Structural Properties: In-Plane Radial Distribution Functions.** The in-plane O−O, H−H, and O−H pair correlation functions given in Figure 3 show additional information for how structured the water could be on the GaN surface. The RDFs are calculated in correspondence to the slabs at several distances from the surface. The slabs are 1 Å in thickness with their centers located at the characteristic peak positions in different regions (as reported in the last section). From all the three RDFs, the first three regions exhibit significant structural orderings extending to the long-range, compared to regions 4, 5, and 6 where a converged bulklike liquid structure is found. Specifically for the O−O RDF, region 1 gives substantial ordering in the long-range, which is commensurate with the confined pattern of O upon the Ga sites observed in the 2D density distributions.[20] In region 2, the long-range structural ordering is reduced, but the first shell coordination number is enhanced, which can be partially attributed to the augmented average HB number per water molecule in this region (Figure 2c). The first shell of region 3 is remarkably undercoordinated, mainly because of the density dilution in this depletion region. It is clear that the GaN substrate perturbs the water structure in the interfacial regions, and the impact is reduced from region 4 (~4.47 Å from the surface) beyond which the water structure converges to the bulk. Our $g_{oo}(r)_{max}$ is 2.97 in region 6, which is in good agreement with that (3.01) in the isotropic SPC-F bulk.

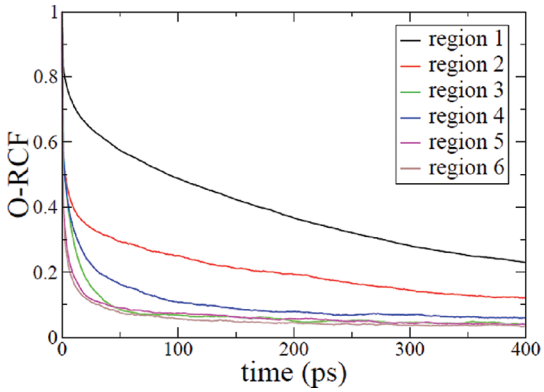


**Figure 4.** Residence correlation functions of oxygen atom of water in different regions.

**C. Dynamic Properties: Residence Correlation Functions.** By basically knowing the structural properties of water on the GaN surface, it is also interesting to understand the relevant dynamic properties of water due to the surface impact. The residence lifetime of molecules in specific layers is an important aspect for the interfacial translational dynamics. We employ a residence correlation function RCF($t$) to account for the residence time of molecules in a particular region of interest.

$$\mathrm{RCF}(t) = \frac{\langle O_w(t) O_w(0) \rangle}{\langle O_w(0) O_w(0) \rangle} \quad (1)$$

As given in eq 1, $O_w(t)$ describes whether an oxygen atom is residing ($O_w(t) = 1$), or not ($O_w(t) = 0$), in the slab of interest at time $t$. Note that the slabs are centered at those characteristic peak positions (as defined above) with the thickness of 1 Å.

Figure 4 shows the RCFs for the six different regions. It can be seen that the correlation function decays much slower in the interfacial region than that in bulk region, indicating that the molecules tend to remain longer when they are closer to the surface. The residence lifetime for regions 1 and 6 is

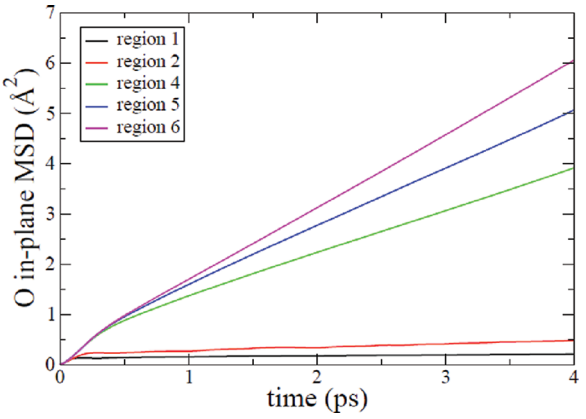


**Figure 5.** O atom of water mean square displacement parallel to the GaN surface in different regions.

**Table 1. Molecular Dipole and H−H Vector Relaxation Time Constants and the in-Plane Oxygen Self-Diffusion Coefficients for Water Located at Different Regions**[a]

| | region 1 | region 2 | region 4 | region 5 | region 6 | bulk |
|---|---|---|---|---|---|---|
| $\tau_{DM}$ (ps) | 20.5 | 61.1 | 6.2 | 5.5 | 4.6 | 4.2 |
| $\tau_{HH}$ (ps) | 15.7 | 95.4 | 4.7 | 4.5 | 3.9 | 3.6 |
| $D_{\|\|}$ (Å$^2$/ps) | 0.006 | 0.024 | 0.216 | 0.294 | 0.36 | 0.285 |

[a] The corresponding bulk data are evaluated from separate calculations by using the isotropic liquid bulk.

approximately 198.8 and 1.5 ps, respectively, as estimated from the time required for RCF($t$) to decay to $1/e$. The pronounced difference demonstrates the effect of the surface confinement which is likely to prevent the molecules from diffusing away from the surface. The observations are consistent with other interfacial systems[6,10,11] such as for water on silica, graphite, and alumina where interfacial residence time is found to be elongated for all cases. Our residence lifetime in region 6 (1.5 ps) is in good agreement with simulation results reported for the SPCE (extended simple point charge model) water in liquid bulk conditions.[6] In addition, we found that the residence lifetime in region 3 is even shorter than that in region 4, which might be caused by the density dilution in region 3 leading to a faster translation in the surface normal direction. The tails of RCFs for the bulklike regions converge only to finite values, demonstrating the fact that a molecule which leaves the respective layer may eventually return to the layer of interest.[11]

**D. Dynamic Properties: In-Plane Diffusions.** It is known that the diffusion of the interfacial water may be slowed down due to its interactions with the substrate.[11,31,32] We are hereby examining the layer-by-layer in-plane translational diffusion of water on GaN surface in detail, by calculating the in-plane MSDs of the oxygen atom.

$$\mathrm{MSD}_{\|} = \langle (x(t) - x(0))^2 + (y(t) - y(0))^2 \rangle \quad (2)$$

The calculations are done by selecting all the possible O atoms that can continuously stay in a specific region of interest up to the maximal time considered; the brackets mean averaging over each atom in a region and a large number of ensembles. Figure 5 shows the in-plane MSDs for different regions (based on the division in Figure 2) up to 4 ps. It can be seen that the translational mobility of water is faster in the region farther from the surface, as expected.

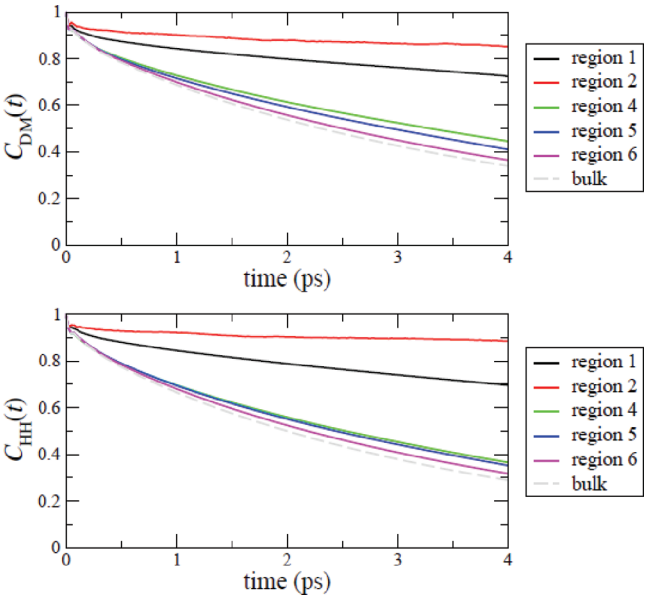


**Figure 6.** Reorientational relaxations for the dipole moment vector (upper panel) and the H−H vector (lower panel) of water in different regions. The relaxations in bulk water are based on separate calculations by using an isotropic liquid bulk.

Note that the MSD for region 3 is not shown in here due to the restricted statistics of molecules that can continuously stay in this thin and dilute layer with relatively short residence lifetime (Figure 4). The in-plane self-diffusion coefficient can be estimated from the derivative of MSD with respect to the time.

$$D_{\|} = \frac{1}{4} \lim_{t \to \infty} \frac{\mathrm{d}}{\mathrm{d}t} \mathrm{MSD}_{\|} \quad (3)$$

We report the $D_{||}$ for different regions (Table 1) by fitting the 1−4 ps portion of the plot to a straight line. Note that the quality of the diffusion coefficient calculation is subject to the maximal time in MSD considered, and in this particular case subject to the lifetime of molecules in a certain region, while the current estimation from 4 ps data, even though limited in terms of its accuracy, can still serve as a good method to compare the translational mobility between different regions. The obtained in-plane diffusion constant in region 1 (0.006 Å$^2$/ps) is around 60 times smaller than that in region 6, demonstrating that the physisorbed water is substantially slowed down by the electrostatic perturbations from the substrate. The isotropic diffusion constant of the SPC-F bulk (0.285 Å$^2$/ps) is also listed, which is in qualitative agreement with the in-plane diffusion constant in region 6.

**E. Dynamic Properties: Reorientational Relaxations.** The rotational diffusion is another important dynamic quantity of interfacial water. To assess this property, we compute the reorientational autocorrelation functions of molecules located at different distances from the surface. The reorientation of two vectors, defined by the molecular dipole moment ($\overrightarrow{\mathrm{DM}}$) and the H−H vector ($\overrightarrow{\mathrm{HH}}$), is considered.

$$C_{\hat{\mu}}(t) = \frac{\langle \hat{\mu}(t) \cdot \hat{\mu}(0) \rangle}{\langle \hat{\mu}(0) \cdot \hat{\mu}(0) \rangle} \quad (4)$$

As shown in eq 4, $\hat{\mu}$ represents the unit vector of $\overrightarrow{\mathrm{DM}}$ and $\overrightarrow{\mathrm{HH}}$ in each case. We calculate the reorientational correlations, $C_{\mathrm{DM}}(t)$


dx.doi.org/10.1021/jp2070166 |J. Phys. Chem. C 2011, 115, 22444–22450

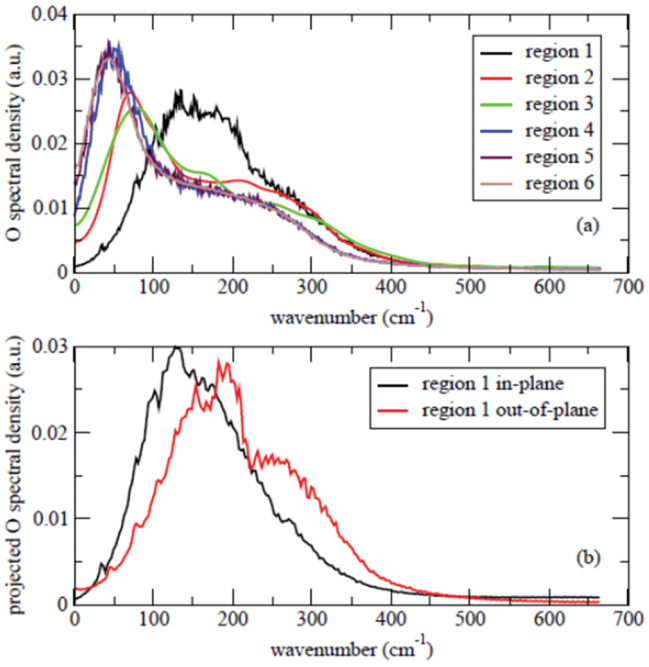


**Figure 7.** (a) O vibrational spectral density in different regions. The spectral densities in regions 2 and 3 have been smoothed by an apodization function. (b) Projections of region 1 O spectral density into in-plane (parallel to the surface) and out-of-plane (perpendicular to the surface) directions.

and $C_{HH}(t)$, for water in different regions by selecting those molecules (molecular location determined by O) that can continuously stay in a layer up to the maximal correlation time considered. The results are given in Figure 6; the data for region 3 are not shown due to the restricted statistics of molecules that can continuously stay in this layer. It is clear that the reorientational relaxations within the hydration layer (region 1 and 2) are significantly slower than those in regions 4, 5, and 6, where convergences to the SPC-F bulk correlation functions are found. The observations are consistent with the rotational relaxations of water on other surfaces,[6,11,33,34] where molecules at interfaces in general reorient more slowly than in the bulk. We further note that for both the molecular dipole and H−H vector relaxations, the correlation functions in region 2 decay even more slowly than those in region 1, demonstrating the effect of the enhanced coordination number in region 2 than in region 1 (Figure 2c) which is expected to slow down the rotational dynamics.

The reorientational relaxation times can be obtained from the analysis of the behavior of $C_{\hat{\mu}}(t)$. In all cases, we find that in the temporal regime, i.e., 1−4 ps, the curves can be reasonably well described by single exponentials ($A\exp(-t/\tau_{\hat{\mu}})$), whose decay constants $\tau_{DM}$ and $\tau_{HH}$ are listed in Table 1. A remarkable rotational anisotropy can be observed especially in the hydration layer. In particular, in region 1 the dipole relaxation is slower than the HH one, which may be caused by the twistinglike libration of molecules in region 1, where O is confined upon the Ga sites with one OH pointing toward the neighboring O,[20] so that only one H pointing away from the surface would have larger mobility that can facilitate the HH relaxation to be faster than the dipole one. However, region 2 gives rise to a HH relaxation slower than that of dipole, which can be attributed to the confined 2D density pattern of H[20] that can lead to a restricted HH rotational diffusion compared to the dipole one. The relaxation times for regions 4, 5, and 6 are reduced and are found to approach the bulk values evaluated from an isotropic SPC-F liquid.

**F. Dynamic Properties: Vibrational Power Spectra.** Vibrational power spectra provide a measure for how the water molecule is coupled with its local environment. Particularly in the low frequency region, the O spectral density gives insightful information for the local HB vibrations. In bulk water, two main features are observed in the O power spectra: a band around 50 cm$^{-1}$, which has been either attributed to the network bending mode[35−37] or the cage effect[38−40] due to the hindered molecular translations, and, in addition, a shoulder centered around 180 cm$^{-1}$, usually being assigned to the HB stretching mode.[36,41]

To investigate how the surface can perturb the HB vibrations, we compute the O spectral density in a layer-by-layer manner. The O vibrational density of states (VDOS) is evaluated via the Fourier transform of the atomic velocity autocorrelation function.

$$\mathrm{VDOS}(\omega) = \int_{-\infty}^{\infty} \mathrm{d}t\, \mathrm{e}^{-i\omega t} \frac{\langle \vec{v}(t)\cdot\vec{v}(0)\rangle}{\langle \vec{v}(0)\cdot\vec{v}(0)\rangle} \qquad (5)$$

The calculations are done by selecting those O atoms that can continuously stay in a region of interest up to the maximal correlation time considered. Figure 7a shows the O spectral density in different regions. It can see that region 4, 5, and 6 give rise to almost converged bulklike spectral profiles by having a peak at around 50 cm$^{-1}$ and a broad shoulder at around 180 cm$^{-1}$, as can be assigned to the vibrational modes described above. The spectra in region 2 and 3 undergo remarkable blue-shift by basically maintaining the two-band spectral line shapes. However, the spectrum of region 1 is even further blue-shifted by displaying a broad peak at around 153 cm$^{-1}$ and a slightly suppressed shoulder at around 260 cm$^{-1}$. There is no doubt that the major peak in region 1 should represent the network bending band, since the diffusion of the interfacial water is largely restricted so that the assignment to a translational mode would be inappropriate. The frequency of the network bending band in region 1 is significantly enhanced compared to the bulk, revealing the effect of the interfacial couplings that can firmly hold the molecules to make a tougher intermolecular bend. The feature of the HB stretching band in region 1 at ∼260 cm$^{-1}$ is less remarkable than that in the bulk, indicating a modulated HB network at the interface.

Further analysis by decomposing the region 1 spectral density into the in-plane and out-of-plane directions (Figure 7b) gives insight into the anisotropy of the HB vibrations at the interface. It can be observed that in the projected in-plane spectrum only a broad network bending band is seen while the shoulder for the HB stretching is absent. The HB stretching band, however, is visible in the out-of-plane projection. It demonstrates that the HB stretching character is active only when the molecule is dynamically linked to the upper liquid, whereas the in-plane O−O stretching is essentially suppressed due to the large electrostatic force acting on the surface O atoms.

## 4. CONCLUSIONS

In summary, we have performed molecular dynamics simulations to investigate various structural and dynamic properties of the interfacial water on the GaN polar surface. The interfacial molecules, especially within the hydration layer including the first

two regions, exhibit enhanced structural ordering and slowed-down dynamics compared to the liquid bulk. The HB density distribution shows a highly structured profile which mimics the atomic density profile. A considerable HB orientational anisotropy is observed within the interfacial regions, where the in-plane HB orientation is dominant within the surface contact bilayer whereas the out-of-plane orientation is the major one for the density depletion region. The physisorbed molecules are found to have the extended long-range ordering along the in-plane direction based on our calculations of RDFs, which is consistent with the structural patterning seen in the 2D density distributions. Further analyses show that when the molecules are closer to the surface, their residence lifetime is elongated by also giving a slower translational diffusion and reorientational relaxations, demonstrating the effect of the surface confinement. Particularly for the reorientational relaxations, the first two regions give rise to significant rotational anisotropies, indicating that there might be two types of water molecules adopting different libration modes within the hydration layer. The low frequency vibrational power spectra have identified a broad network bending band for the interfacial region which is blue-shifted compared to the counterpart in the liquid bulk. The HB stretching at the interface is found to have substantial anisotropy where the stretching mode is essentially suppressed in the in-plane projection and only active when the physisorbed molecules are dynamically linked to the upper liquid.

We found that the GaN polar surface has created an interfacial region within a few molecular dimensions from the substrate, where the major forces dominating this region are the water/substrate electrostatic couplings and the water/water interactions. The anisotropy is essential in this interfacial region where the structural arrangement, molecular orientations, HB orientations, rotational relaxations, and intermolecular vibrations are considerably different from the isotropic bulk. Such findings would be useful to study the nonlinear optical processes of water molecules in contact with the GaN surface,[42] where the interfacial water anisotropy would play an important role. The study could be further related to the photocatalytic activities of GaN that can promote $H_2$ generation from the aqueous solutions[19,21−23], in which case more advanced simulations (i.e., first principle MD) relevant to the water surface chemistry on GaN can possibly be derived from our current classical molecular dynamics.

## AUTHOR INFORMATION

### Corresponding Author

*E-mail zhengtan@pub.iams.sinica.edu.tw (O.Z.T.); jlkuo@pub.iams.sinica.edu.tw (J.-L.K.).

## ACKNOWLEDGMENT

This work is supported in part under Academia Sinica Research Program on NanoScience and Nano Technology and National Science Council (NSC98-2113-M-001-029-MY3) of Taiwan. We thank Dr. Chien-Cheng Chen, Dr. Yu-Chieh Wen, and Prof. Chi-Kuang Sun of Natinal Taiwan University for their encouragement and helpful discussions on the computational work.

## REFERENCES

(1) Antognozzi, M.; Humphris, A. D. L.; Miles, M. J. *Appl. Phys. Lett.* **2001**, *78* (3), 300.
(2) Fenter, P.; Sturchio, N. C. *Prog. Surf. Sci.* **2004**, *77* (5−8), 171.
(3) Hussain, M.; Anwar, J. *J. Am. Chem. Soc.* **1999**, *121* (37), 8583.
(4) Malikova, N.; Cadene, A.; Marry, V.; Dubois, E.; Turq, P. *J. Phys. Chem. B* **2006**, *110* (7), 3206.
(5) Mamontov, E.; Wesolowski, D. J.; Vlcek, L.; Cummings, P. T.; Rosenqvist, J.; Wang, W.; Cole, D. R. *J. Phys. Chem. C* **2008**, *112* (32), 12334.
(6) Argyris, D.; Tummala, N. R.; Striolo, A.; Cole, D. R. *J. Phys. Chem. C* **2008**, *112* (35), 13587.
(7) Giovambattista, N.; Rossky, P. J.; Debenedetti, P. G. *J. Phys. Chem. B* **2009**, *113* (42), 13723.
(8) Argyris, D.; Cole, D. R.; Striolo, A. *Langmuir* **2009**, *25* (14), 8025.
(9) Wang, J. W.; Kalinichev, A. G.; Kirkpatrick, R. J. *J. Phys. Chem. C* **2009**, *113* (25), 11077.
(10) Argyris, D.; Ho, T. A.; Cole, D. R.; Striolo, A. *J. Phys. Chem. C* **2011**, *115* (5), 2038.
(11) Argyris, D.; Cole, D. R.; Striolo, A. *J. Phys. Chem. C* **2009**, *113* (45), 19591.
(12) Gordillo, M. C.; Marti, J. *J. Phys. Chem. B* **2010**, *114* (13), 4583.
(13) Pearton, S. J.; Ren, F.; Wang, Y. L.; Chu, B. H.; Chen, K. H.; Chang, C. Y.; Lim, W.; Lin, J. S.; Norton, D. P. *Prog. Mater. Sci.* **2010**, *55* (1), 1.
(14) Lee, D. S.; Lee, J. H.; Lee, Y. H.; Lee, D. D. *Sens. Actuators, B* **2003**, *89* (3), 305.
(15) Lorenz, P.; Gutt, R.; Haensel, T.; Himmerlich, M.; Schaefer, J. A.; Krischok, S. *Phys. Status Solidi C* **2010**, *7* (2), 169.
(16) Stutzmann, M.; Steinhoff, G.; Eickhoff, M.; Ambacher, O.; Nebel, C. E.; Schalwig, J.; Neuberger, R.; Muller, G. *Diamond Relat. Mater.* **2002**, *11* (3−6), 886.
(17) Shen, X.; Allen, P. B.; Hybertsen, M. S.; Muckerman, J. T. *J. Phys. Chem. C* **2009**, *113* (9), 3365.
(18) Shen, X. A.; Small, Y. A.; Wang, J.; Allen, P. B.; Fernandez-Serra, M. V.; Hybertsen, M. S.; Muckerman, J. T. *J. Phys. Chem. C* **2010**, *114* (32), 13695.
(19) Chen, P. T.; Sun, C. L.; Hayashi, M. *J. Phys. Chem. C* **2010**, *114* (42), 18228.
(20) Tan, O. Z.; Wu, M. C. H.; Chihaia, V.; Kuo, J. L. *J. Phys. Chem. C* **2011**, *115* (23), 11684.
(21) Fujii, K.; Karasawa, T. K.; Ohkawa, K. *Jpn. J. Appl. Phys., Part 2* **2005**, *44* (16−19), L543.
(22) Liu, S. Y.; Sheu, J. K.; Tseng, C. K.; Ye, J. C.; Chang, K. H.; Lee, M. L.; Lai, W. C. *J. Electrochem. Soc.* **2010**, *157* (2), B266.
(23) Fujii, K.; Ohkawa, K. *J. Electrochem. Soc.* **2006**, *153* (3), A468.
(24) Lima, E. R. A.; Bostrom, M.; Horinek, D.; Biscaia, E. C.; Kunz, W.; Tavares, F. W. *Langmuir* **2008**, *24* (8), 3944.
(25) Berendsen, H. J. C.; Postma, J. P. M.; van Gunsteren, W. F.; Hermans, J. Interaction models for water in relation to protein hydration. In *Intermolecular Forces*; Pullman, B., Ed.; D. Reidel: Amsterdam, The Netherlands, 1981; p 331.
(26) Teleman, O.; Jönsson, B.; Engström, S. *Mol. Phys.* **1987**, *60* (1), 193.
(27) Gale, J. D. *J. Chem. Soc., Faraday Trans.* **1997**, *93* (4), 629.
(28) Marti, J.; Padro, J. A.; Guardia, E. *J. Chem. Phys.* **1996**, *105* (2), 639.
(29) Marti, J.; Nagy, G.; Gordillo, M. C.; Guardia, E. *J. Chem. Phys.* **2006**, *124* (9), 094703.
(30) Liu, L. M.; Krack, M.; Michaelides, A. *J. Chem. Phys.* **2009**, *130* (23), 234702.
(31) Bonnaud, P. A.; Coasne, B.; Pellenq, R. J. M. *J. Phys.: Condens. Matter* **2010**, *22* (28), 284110.
(32) Leng, Y. S.; Cummings, P. T. *Phys. Rev. Lett.* **2005**, *94* (2), 026101.
(33) Bhide, S. Y.; Berkowitz, M. L. *J. Chem. Phys.* **2005**, *123* (22), 224702.
(34) Bhide, S. Y.; Berkowitz, M. L. *J. Chem. Phys.* **2006**, *125* (9), 094713.

(35) Walrafen, G. E.; Chu, Y. C.; Piermarini, G. J. *J. Phys. Chem.* **1996**, *100* (24), 10363.
(36) Walrafen, G. E.; Fisher, M. R.; Hokmabadi, M. S.; Yang, W. H. *J. Chem. Phys.* **1986**, *85* (12), 6970.
(37) Walrafen, G. E.; Hokmabadi, M. S.; Yang, W. H.; Chu, Y. C.; Monosmith, B. *J. Phys. Chem.* **1989**, *93* (8), 2909.
(38) Padro, J. A.; Marti, J. *J. Chem. Phys.* **2003**, *118* (1), 452.
(39) De Santis, A.; Ercoli, A.; Rocca, D. *J. Chem. Phys.* **2004**, *120* (3), 1657.
(40) Padro, J. A.; Marti, J. *J. Chem. Phys.* **2004**, *120* (3), 1659.
(41) Krishnamurthy, S.; Bansil, R.; Wiafeakenten, J. *J. Chem. Phys.* **1983**, *79* (12), 5863.
(42) Kanemaru, H.; Nosaka, Y.; Hirako, A.; Ohkawa, K.; Kobayashi, T.; Tokunaga, E. *Opt. Rev.* **2010**, *17* (3), 352.